TOWARDS FASTER AND STABILIZED GAN TRAINING FOR HIGH-FIDELITY FEW-SHOT IMAGE SYNTHESIS

Bingchen Liu[1,2], **Yizhe Zhu**[2], **Kunpeng Song**[1,2], **Ahmed Elgammal**[1,2]
[1]Playform - Artrendex Inc., USA
[2]Department of Computer Science, Rutgers University
{bingchen.liu,yizhe.zhu,kunpeng.song}@rutgers.edu
elgammal@artrendex.com

ABSTRACT

Training Generative Adversarial Networks (GAN) on high-fidelity images usually requires large-scale GPU-clusters and a vast number of training images. In this paper, we study the few-shot image synthesis task for GAN with minimum computing cost. We propose a light-weight GAN structure that gains superior quality on 1024×1024 resolution. Notably, the model converges from scratch with just a few hours of training on a single RTX-2080 GPU, and has a consistent performance, even with less than 100 training samples. Two technique designs constitute our work, a skip-layer channel-wise excitation module and a self-supervised discriminator trained as a feature-encoder. With thirteen datasets covering a wide variety of image domains [1], we show our model's superior performance compared to the state-of-the-art StyleGAN2, when data and computing budget are limited.

1 INTRODUCTION

The fascinating ability to synthesize images using the state-of-the-art (SOTA) Generative Adversarial Networks (GANs) (Goodfellow et al., 2014) display a great potential of GANs for many intriguing real-life applications, such as image translation, photo editing, and artistic creation. However, expensive computing cost and the vast amount of required training data limit these SOTAs in real applications with only small image sets and low computing budgets.

In real-life scenarios, the available samples to train a GAN can be minimal, such as the medical images of a rare disease, a particular celebrity's portrait set, and a specific artist's artworks. Transfer-learning with a pre-trained model (Mo et al., 2020; Wang et al., 2020) is one solution for the lack of training images. Nevertheless, there is no guarantee to find a compatible pre-training dataset. Furthermore, if not, fine-tuning probably leads to even worse performance (Zhao et al., 2020).

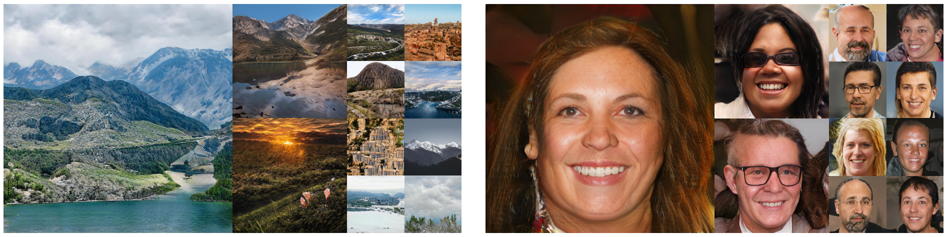

Figure 1: **Synthetic results on** 1024^2 **resolution** of our model, trained from scratch on single RTX 2080-Ti GPU, with only 1000 images. Left: 20 hours on Nature photos; Right: 10 hours on FFHQ.

In a recent study, it was highlighted that in art creation applications, most artists prefers to train their models from scratch based on their own images to avoid biases from fine-tuned pre-trained model. Moreover, It was shown that in most cases artists want to train their models with datasets of less than

[1] The datasets and code are available at: https://github.com/odegeasslbc/FastGAN-pytorch

100 images (Elgammal et al., 2020). Dynamic data-augmentation (Karras et al., 2020a; Zhao et al., 2020) smooths the gap and stabilizes GAN training with fewer images. However, the computing cost from the SOTA models such as StyleGAN2 (Karras et al., 2020b) and BigGAN (Brock et al., 2019) remain to be high, especially when trained with the image resolution on 1024×1024.

In this paper, our goal is to learn an unconditional GAN on high-resolution images, with low computational cost and few training samples. As summarized in Fig. 2, these training conditions expose the model to a high risk of overfitting and mode-collapse (Arjovsky & Bottou, 2017; Zhang & Khoreva, 2018). To train a GAN given the demanding training conditions, we need a generator (G) that can learn fast, and a discriminator (D) that can continuously provide useful signals to train G. To address these challenges, we summarize our contribution as:

- We design the Skip-Layer channel-wise Excitation (SLE) module, which leverages low-scale activations to revise the channel responses on high-scale feature-maps. SLE allows a more robust gradient flow throughout the model weights for faster training. It also leads to an automated learning of a style/content disentanglement like StyleGAN2.
- We propose a self-supervised discriminator D trained as a feature-encoder with an extra decoder. We force D to learn a more descriptive feature-map covering more regions from an input image, thus yielding more comprehensive signals to train G. We test multiple self-supervision strategies for D, among which we show that auto-encoding works the best.
- We build a computational-efficient GAN model based on the two proposed techniques, and show the model's robustness on multiple high-fidelity datasets, as demonstrated in Fig. 1.

2 Related Works

Speed up the GAN training: Speeding up the training of GAN has been approached from various perspectives. Ngxande et al. propose to reduce the computing time with depth-wise convolutions. Zhong et al. adjust the GAN objective into a min-max-min problem for a shorter optimization path. Sinha et al. suggest to prepare each batch of training samples via a coreset selection, leverage the better data preparation for a faster convergence. However, these methods only bring a limited improvement in training speed. Moreover, the synthesis quality is not advanced within the shortened training time.

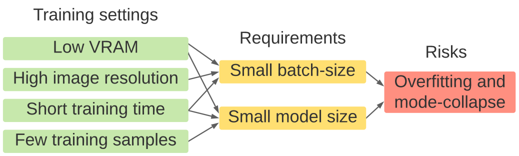

Figure 2: The causes and challenges for training GAN in our studied conditions.

Train GAN on high resolution: High-resolution training for GAN can be problematic. Firstly, the increased model parameters lead to a more rigid gradient flow to optimize G. Secondly, the target distribution formed by the images on 1024×1024 resolution is super sparse, making GAN much harder to converge. Denton et al. (2015); Zhang et al. (2017); Huang et al. (2017); Wang et al. (2018); Karras et al. (2019); Karnewar & Wang (2020); Karras et al. (2020b); Liu et al. (2021) develop the multi-scale GAN structures to alleviate the gradient flow issue, where G outputs images and receives feedback from several resolutions simultaneously. However, all these approaches further increase the computational cost, consuming even more GPU memory and training time.

Stabilize the GAN training: Mode-collapse on G is one of the big challenges when training GANs. And it becomes even more challenging given fewer training samples and a lower computational budget (a smaller batch-size). As D is more likely to be overfitting on the datasets, thus unable to provide meaningful gradients to train G (Gulrajani et al., 2017).

Prior works tackle the overfitting issue by seeking a good regularization for D, including different objectives (Arjovsky et al., 2017; Lim & Ye, 2017; Tran et al., 2017); regularizing the gradients (Gulrajani et al., 2017; Mescheder et al., 2018); normalizing the model weights (Miyato et al., 2018); and augmenting the training data (Karras et al., 2020a; Zhao et al., 2020). However, the effects of these methods degrade fast when the training batch-size is limited, since appropriate batch statistics can hardly be calculated for the regularization (normalization) over the training iterations.

Meanwhile, self-supervision on D has been shown to be an effective method to stabilize the GAN training as studied in Tran et al. (2019); Chen et al. (2019). However, the auxiliary self-supervision tasks in prior works have limited using scenario and image domain. Moreover, prior works only studied on low resolution images (32^2 to 128^2), and without a computing resource limitation.

3 METHOD

We adopt a minimalistic design for our model. In particular, we use a single conv-layer on each resolution in G, and apply only three (input and output) channels for the conv-layers on the high resolutions ($\geq 512 \times 512$) in both G and D. Fig. 3 and Fig. 4 illustrate the model structure for our G and D, with descriptions of the component layers and forward flow. These structure designs make our GAN much smaller than SOTA models and substantially faster to train. Meanwhile, our model remains robust on small datasets due to its compact size with the two proposed techniques.

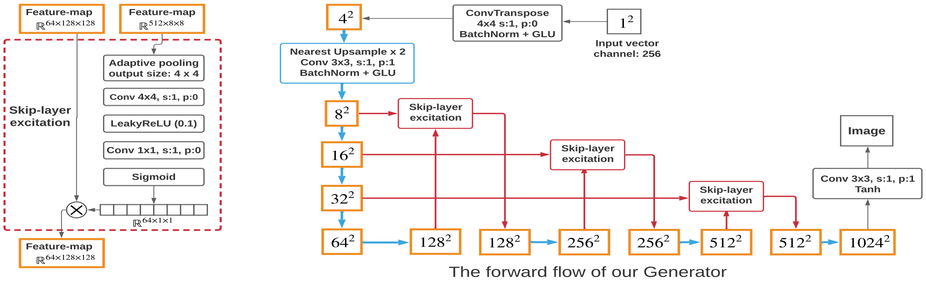
Feature-map $\mathbb{R}^{64\times128\times128}$
Feature-map $\mathbb{R}^{512\times8\times8}$
Skip-layer excitation
Adaptive pooling output size: 4 x 4
Conv 4x4, s:1, p:0
LeakyReLU (0.1)
Conv 1x1, s:1, p:0
Sigmoid
$\mathbb{R}^{64\times1\times1}$
Feature-map $\mathbb{R}^{64\times128\times128}$
4^2
ConvTranspose 4x4 s:1, p:0 BatchNorm + GLU
1^2
Input vector channel: 256
Nearest Upsample x 2 Conv 3x3, s:1, p:1 BatchNorm + GLU
8^2
Skip-layer excitation
16^2
Skip-layer excitation
32^2
Skip-layer excitation
Image
Conv 3x3, s:1, p:1 Tanh
64^2
128^2
128^2
256^2
256^2
512^2
512^2
1024^2

The forward flow of our Generator

Figure 3: The structure of the skip-layer excitation module and the Generator. Yellow boxes represent feature-maps (we show the spatial size and omit the channel number), blue box and blue arrows represent the same up-sampling structure, red box contains the SLE module as illustrated on the left.

3.1 SKIP-LAYER CHANNEL-WISE EXCITATION

For synthesizing higher resolution images, the generator G inevitably needs to become deeper, with more conv-layers, in concert with the up-sampling needs. A deeper model with more convolution layers leads to a longer training time of GAN, due to the increased number of model parameters and a weaker gradient flow through G (Zhang et al., 2017; Karras et al., 2018; Karnewar & Wang, 2020). To better train a deep model, He et al. design the Residual structure (ResBlock), which uses a skip-layer connection to strengthen the gradient signals between layers. However, while ResBlock has been widely used in GAN literature (Wang et al., 2018; Karras et al., 2020b), it also increases the computation cost.

We reformulate the skip-connection idea with two unique designs into the *Skip-Layer Excitation* module (SLE). First, ResBlock implements skip-connection as an element-wise addition between the activations from different conv-layers. It requires the spatial dimensions of the activations to be the same. Instead of addition, we apply channel-wise multiplications between the activations, eliminating the heavy computation of convolution (since one side of the activations now has a spatial dimension of 1^2). Second, in prior GAN works, skip-connections are only used within the same resolution. In contrast, we perform skip-connection between resolutions with a much longer range (e.g., 8^2 and 128^2, 16^2 and 256^2), since an equal spatial-dimension is no longer required. The two designs make SLE inherits the advantages of ResBlock with a shortcut gradient flow, meanwhile without an extra computation burden.

Formally, we define the Skip-Layer Excitation module as:

$$\mathbf{y} = \mathcal{F}(\mathbf{x}_{low}, \{\mathbf{W}_i\}) \cdot \mathbf{x}_{high} \tag{1}$$

Here $\mathbf{x}$ and $\mathbf{y}$ are the input and output feature-maps of the SLE module, the function $\mathcal{F}$ contains the operations on $\mathbf{x}_{low}$, and $\mathbf{W}_i$ indicates the module weights to be learned. The left panel in Fig. 3 shows an SLE module in practice, where $\mathbf{x}_{low}$ and $\mathbf{x}_{high}$ are the feature-maps at 8×8 and 128×128 resolution respectively. An adaptive average-pooling layer in $\mathcal{F}$ first down-samples $\mathbf{x}_{low}$ into 4×4

along the spatial-dimensions, then a conv-layer further down-samples it into 1×1. A LeakyReLU is used to model the non-linearity, and another conv-layer projects $\mathbf{x}_{low}$ to have the same channel size as $\mathbf{x}_{high}$. Finally, after a gating operation via a Sigmoid function, the output from $\mathcal{F}$ multiplies $\mathbf{x}_{high}$ along the channel dimension, yielding $\mathbf{y}$ with the same shape as $\mathbf{x}_{high}$.

SLE partially resembles the Squeeze-and-Excitation module (SE) proposed by Hu et al.. However, SE operates within one feature-map as a self-gating module. In comparison, SLE performs between feature-maps that are far away from each other. While SLE brings the benefit of channel-wise feature re-calibration just like SE, it also strengthens the whole model's gradient flow like ResBlock. The channel-wise multiplication in SLE also coincides with Instance Normalization (Ulyanov et al., 2016; Huang & Belongie, 2017), which is widely used in style-transfer. Similarly, we show that SLE enables G to automatically disentangle the content and style attributes, just like StyleGAN (Karras et al., 2019). As SLE performs on high-resolution feature-maps, altering these feature-maps is shown to be more likely to change the style attributes of the generated image (Karras et al., 2019; Liu et al., 2021). By replacing x_{low} in SLE from another synthesized sample, our G can generate an image with the content unchanged, but in the same style of the new replacing image.

3.2 Self-supervised discriminator

Our approach to provide a strong regularization for D is surprisingly simple. We treat D as an encoder and train it with small decoders. Such auto-encoding training forces D to extract image features that the decoders can give good reconstructions. The decoders are optimized together with D on a simple reconstruction loss, which is only trained on real samples:

$$\mathcal{L}_{recons} = \mathbb{E}_{\mathbf{f} \sim D_{encode}(x),\, x \sim I_{real}} [||\mathcal{G}(\mathbf{f}) - \mathcal{T}(x)||], \tag{2}$$

where $\mathbf{f}$ is the intermediate feature-maps from D, the function $\mathcal{G}$ contains the processing on $\mathbf{f}$ and the decoder, and the function $\mathcal{T}$ represents the processing on sample x from real images I_{real}.

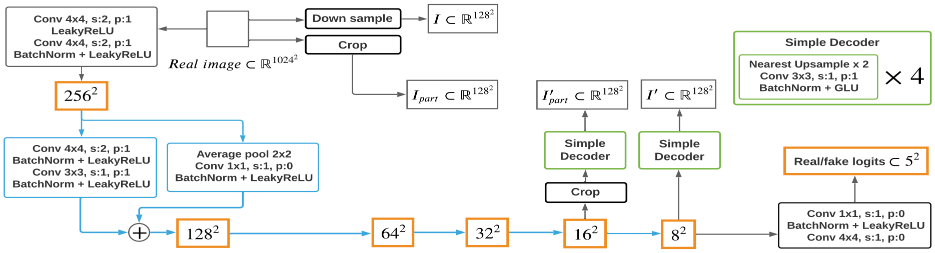

Figure 4: The structure and the forward flow of the Discriminator. Blue box and arrows represent the same residual down-sampling structure, green boxes mean the same decoder structure.

Our self-supervised D is illustrated in Fig. 4, where we employ two decoders for the feature-maps on two scales: $\mathbf{f}_1$ on 16^2 and $\mathbf{f}_2$ on 8^2 . The decoders only have four conv-layers to produce images at 128×128 resolution, causing little extra computations (much less than other regularization methods). We randomly crop $\mathbf{f}_1$ with $\frac{1}{8}$ of its height and width, then crop the real image on the same portion to get I_{part}. We resize the real image to get I. The decoders produce I'_{part} from the cropped $\mathbf{f}_1$, and I' from $\mathbf{f}_2$. Finally, D and the decoders are trained together to minimize the loss in eq. 2, by matching I'_{part} to I_{part} and I' to I.

Such reconstructive training makes sure that D extracts a more comprehensive representation from the inputs, covering both the overall compositions (from $\mathbf{f}_2$) and detailed textures (from $\mathbf{f}_1$). Note that the processing in $\mathcal{G}$ and $\mathcal{T}$ are not limited to cropping; more operations remain to be explored for better performance. The auto-encoding approach we employ is a typical method for self-supervised learning, which has been well recognized to improve the model robustness and generalization ability (He et al., 2020; Hendrycks et al., 2019; Jing & Tian, 2020; Goyal et al., 2019). In the context of GAN, we find that a regularized D via self-supervision training strategies significantly improves the synthesis quality on G, among which auto-encoding brings the most performance boost.

Although our self-supervision strategy for D comes in the form of an auto-encoder (AE), this approach is fundamentally different from works trying to combine GAN and AE (Larsen et al., 2016;

Guo et al., 2019; Zhao et al., 2016; Berthelot et al., 2017). The latter works mostly train G as a decoder on a learned latent space from D, or treat the adversarial training with D as an supplementary loss besides AE's training. In contrast, our model is a pure GAN with a much simpler training schema. The auto-encoding training is only for regularizing D, where G is not involved.

In sum, we employ the hinge version of the adversarial loss (Lim & Ye (2017); Tran et al. (2017)) to iteratively train our D and G. We find the different GAN losses make little performance difference, while hinge loss computes the fastest:

$$\mathcal{L}_D = - \mathbb{E}_{x \sim I_{real}}[min(0, -1 + D(x))] - \mathbb{E}_{\hat{x} \sim G(z)}[min(0, -1 - D(\hat{x})] + \mathcal{L}_{recons} \tag{3}$$

$$\mathcal{L}_G = - \mathbb{E}_{z \sim \mathcal{N}}[D(G(z))], \tag{4}$$

4 Experiment

Datasets: We conduct experiments on multiple datasets with a wide range of content categories. On 256×256 resolution, we test on Animal-Face Dog and Cat (Si & Zhu, 2011), 100-Shot-Obama, Panda, and Grumpy-cat (Zhao et al., 2020). On 1024×1024 resolution, we test on Flickr-Face-HQ (FFHQ) (Karras et al., 2019), Oxford-flowers (Nilsback & Zisserman, 2006), art paintings from WikiArt (wikiart.org), photographs on natural landscape from Unsplash (unsplash.com), Pokemon (pokemon.com), anime face, skull, and shell. These datasets are designed to cover images with different characteristics: photo realistic, graphic-illustration, and art-like images.

Metrics: We use two metrics to measure the models' synthesis performance: 1) Fréchet Inception Distance (FID) (Heusel et al., 2017) measures the overall semantic realism of the synthesized images. For datasets with less than 1000 images (most only have 100 images), we let G generate 5000 images and compute FID between the synthesized images and the whole training set. 2) Learned perceptual similarity (LPIPS) (Zhang et al., 2018) provides a perceptual distance between two images. We use LPIPS to report the reconstruction quality when we perform latent space back-tracking on G given real images, and measure the auto-encoding performance. We find it unnecessary to involve other metrics, as FID is unlikely to be inconsistent with the others, given the notable performance gap between our model and the compared ones. For all the testings, we train the models 5 times with random seeds, and report the highest scores. The relative error is less than five percent on average.

Compared Models: We compare our model with: 1) the state-of-the-art (SOTA) unconditional model, StyleGAN2, 2) a baseline model ablated from our proposed one. Note that we adopt StyleGAN2 with recent studies from (Karras et al., 2020a; Zhao et al., 2020), including the model configuration and differentiable data-augmentation, for the best training on few-sample datasets. Since StyleGAN2 requires much more computing-cost (cc) to train, we derive an extra baseline model. In sum, we compare our model with StyleGAN2 on the absolute image synthesis quality regardless of cc, and use the baseline model for the reference within a comparable cc range.

The baseline model is the strongest performer that we integrated from various GAN techniques based on DCGAN (Radford et al., 2015): 1) spectral-normalization (Miyato et al., 2018), 2) exponential-moving-average (Yazıcı et al., 2018) optimization on G, 3) differentiable-augmentation, 4) GLU (Dauphin et al., 2017) instead of ReLU in G. We build our model upon the baseline with the two proposed techniques: the skip-layer excitation module and the self-supervised discriminator.

Table 1: Computational cost comparison of the models.

		StyleGAN2@0.25	StyleGAN2@0.5	StyleGAN2	Baseline	Ours
Resolution: 256^2 Batch-size: 8	Training time (hour / 10k iter)	1	1.8	3.8	0.7	1
	Training vram (GB)	7	16	18	5	6.5
	Model parameters (million)	27.557	45.029	108.843	44.359	47.363
Resolution: 1024^2 Batch-size: 8	Training time (hour / 10k iter)	3.6	5	7	1.3	1.7
	Training vram (GB)	12	23	36	9	10
	Model parameters (million)	27.591	45.15	109.229	44.377	47.413

Table. 1 presents the normalized cc figures of the models on Nvidia's RTX 2080-Ti GPU, implemented using PyTorch (Paszke et al., 2017). Importantly, the slimed StyleGAN2 with $\frac{1}{4}$ parameters cannot converge on the tested datasets at 1024^2 resolution. We compare to the StyleGAN2 with $\frac{1}{2}$ parameters (if not specifically mentioned) in the following experiments.

4.1 Image synthesis performance

Few-shot generation: Collecting large-scale image datasets are expensive, or even impossible, for a certain character, a genre, or a topic. On those few-shot datasets, a data-efficient model becomes especially valuable for the image generation task. In Table. 2 and Table. 3, we show that our model not only achieves superior performance on the few-shot datasets, but also much more computational-efficient than the compared methods. We save the checkpoints every 10k iterations during training and report the best FID from the checkpoints (happens at least after 15 hours of training for StyleGAN2 on all datasets). Among the 12 datasets, our model performs the best on 10 of them.

Please note that, due to the VRAM requirement for StyleGAN2 when trained on 1024^2 resolution, we have to train the models in Table. 3 on a RTX TITAN GPU. In practice, 2080-TI and TITAN share a similar performance, and our model runs the same time on both GPUs.

Table 2: FID comparison at 256^2 resolution on few-sample datasets.

			Animal Face - Dog	Animal Face - Cat	Obama	Panda	Grumpy-cat
Image number			389	160	100	100	100
Training time on one RTX 2080-Ti	20 hour	StyleGAN2	58.85	42.44	46.87	12.06	27.08
		StyleGAN2 finetune	61.03	46.07	**35.75**	14.5	29.34
	5 hour	Baseline	108.19	150.3	62.74	15.4	42.13
		Baseline+Skip	94.21	72.97	52.50	14.39	38.17
		Baseline+decode	56.25	36.74	44.34	10.12	29.38
		Ours (B+Skip+decode)	**50.66**	**35.11**	41.05	**10.03**	**26.65**

Training from scratch vs. fine-tuning: Fine-tuning from a pre-trained GAN (Mo et al., 2020; Noguchi & Harada, 2019; Wang et al., 2020) has been the go-to method for the image generation task on datasets with few samples. However, its performance highly depends on the semantic consistency between the new dataset and the available pre-trained model. According to Zhao et al., fine-tuning performs worse than training from scratch in most cases, when the content from the new dataset strays away from the original one. We confirm the limitation of current fine-tuning methods from Table. 2 and Table. 3, where we fine-tune StyleGAN2 trained on FFHQ use the Freeze-D method from Mo et al.. Among all the tested datasets, only Obama and Skull favor the fine-tuning method, making sense since the two sets share the most similar contents to FFHQ.

Module ablation study: We experiment with the two proposed modules in Table. 2, where both SLE (skip) and decoding-on-D (decode) can separately boost the model performance. It shows that the two modules are orthogonal to each other in improving the model performance, and the self-supervised D makes the biggest contribution. Importantly, the baseline model and StyleGAN2 diverge fast after the listed training time. In contrast, our model is less likely to mode collapse among the tested datasets. Unlike the baseline model which usually model-collapse after trained for 10 hours, our model maintains a good synthesis quality and won't collapse even after trained for 20 hours. We argue that it is the decoding regularization on D that prevents the model from divergence.

Table 3: FID comparison at 1024^2 resolution on few-sample datasets.

			Art Paintings	FFHQ	Flower	Pokemon	Anime Face	Skull	Shell
Image number			1000	1000	1000	800	120	100	60
Training time on one RTX TITAN	24 hour	StyleGAN2	74.56	25.66	45.23	190.23	152.73	127.98	241.37
		StyleGAN2 finetune	N/A	N/A	36.72	60.12	61.23	**107.68**	220.45
	8 hour	Baseline	62.27	38.35	42.25	67.86	101.23	186.45	202.32
		Ours	**45.08**	**24.45**	**25.66**	**57.19**	**59.38**	130.05	**155.47**

Table 4: FID comparison at 1024^2 resolution on datasets with more images.

Model	Dataset	Art Paintings			FFHQ				Nature Photograph		
	Image number	2k	5k	10k	2k	5k	10k	70k	2k	5k	10k
StyleGAN2		70.02	48.36	**41.23**	**18.38**	**10.45**	**7.86**	**4.4**	67.12	**41.47**	**39.05**
Baseline		60.02	51.23	49.38	36.45	27.86	25.12	17.62	71.47	66.05	62.28
Ours		**44.57**	**43.27**	42.53	19.01	17.93	16.45	12.38	**52.47**	45.07	43.65

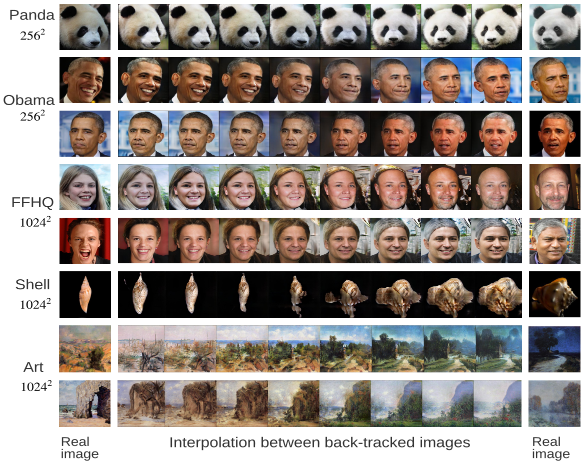

Figure 6: Latent space back-tracking and interpolation.

Table 5: LPIPS of back-tracking with G

	Cat	Dog	FFHQ	Art
Resolution	256		1024	
Baseline @ 20k iter	2.113	2.073	2.589	2.916
Baseline @ 40k iter	2.513	2.171	2.583	2.812
Ours @ 40k iter	**1.821**	**1.918**	2.425	2.624
Ours @ 80k iter	1.897	1.986	**2.342**	**2.601**

Table 6: FID of self-supervisions for D

	Art paintings	Nature photos
a. contrastive loss	47.14	57.04
b. predict aspect ratio	49.21	59.22
c. auto-encoding	**42.53**	**43.65**
d. a+b	46.02	54.23
e. a+b+c	44.21	47.65

Training with more images: For more thorough evaluation, we also test our model on datasets with more sufficient training samples, as shown in Table. 4. We train the full StyleGAN2 for around five days on the Art and Photograph dataset with a batch-size of 16 on two TITAN RTX GPUs, and use the latest official figures on FFHQ from Zhao et al.. Instead, we train our model for only 24 hours, with a batch-size of 8 on a single 2080-Ti GPU. Specifically, for FFHQ with all 70000 images, we train our model with a larger batch-size of 32, to reflect an optimal performance of our model.

In this test, we follow the common practice of computing FID by generating 50k images and use the whole training set as the reference distribution. Note that StyleGAN2 has more than double the parameters compared to our model, and trained with a much larger batch-size on FFHQ. These factors contribute to its better performances when given enough training samples and computing power. Meanwhile, our model keeps up well with StyleGAN2 across all testings with a considerably lower computing budget, showing a compelling performance even on larger-scale datasets, and a consistent performance boost over the baseline model.

Qualitative results: The advantage of our model becomes more clear from the qualitative comparisons in Fig. 5. Given the same batch-size and training time, StyleGAN2 either converges slower or suffers from mode collapse. In contrast, our model consistently generates satisfactory images. Note that the best results from our model on Flower, Shell, and Pokemon only take three hours' training, and for the rest three datasets, the best performance is achieved at training for eight hours. For StyleGAN2 on "shell", "anime face", and "Pokemon", the images shown in Fig. 5 are already from the best epoch, which they match the scores in Table. 2 and Table. 3. For the rest of the datasets, the quality increase from StyleGAN2 is also limited given more training time.

4.2 More Analysis and Applications

Testing mode collapse with back-tracking: From a well trained GAN, one can take a real image and invert it back to a vector in the latent space of G, thus editing the image's content by altering the back-tracked vector. Despite the various back-tracking methods (Zhu et al., 2016; Lipton & Tripathi, 2017; Zhu et al., 2020; Abdal et al., 2019), a well generalized G is arguably as important for the good inversions. To this end, we show that our model, although trained on limited image samples, still gets a desirable performance on real image back-tracking.

In Table 5, we split the images from each dataset with a training/testing ratio of 9:1, and train G on the training set. We compute a reconstruction error between all the images from the testing set and their inversions from G, after the same update of 1000 iterations on the latent vectors (to prevent the vectors from being far off the normal distribution). The baseline model's performance is getting worse with more training iterations, which reflects mode-collapse on G. In contrast, our model gives better reconstructions with consistent performance over more training iterations. Fig. 6 presents the back-tracked examples (left-most and right-most samples in the middle panel) given the real images.

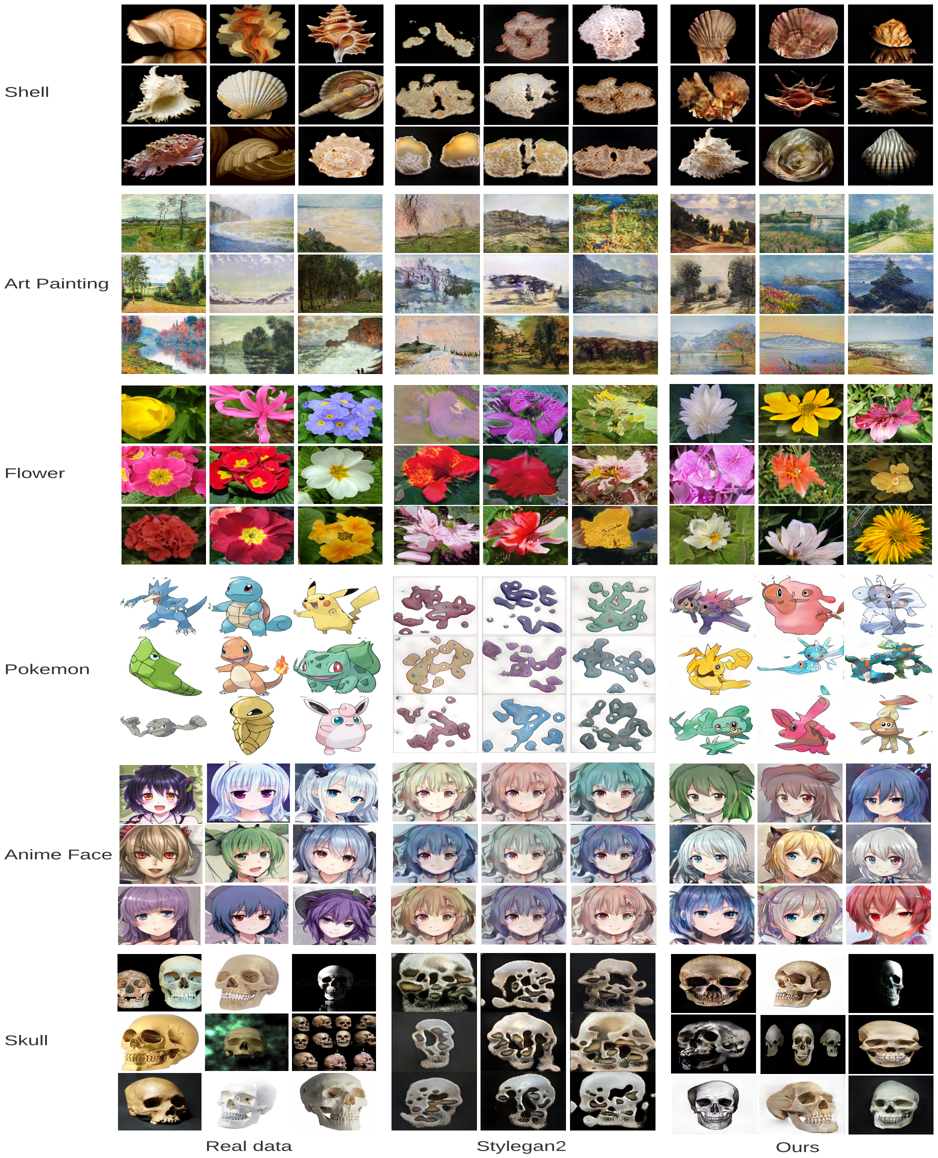

Figure 5: **Qualitative comparison between our model and StyleGAN2** on 1024^2 resolution datasets. The left-most panel shows the training images, and the right two panels show the un-curated samples from StyleGAN2 and our model. Both models are trained from scratch for 10 hours with a batch-size of 8. The samples are generated from the checkpoint with the lowest FID.

The smooth interpolations from the back-tracked latent vectors also suggest little mode-collapse of our G (Radford et al., 2015; Zhao et al., 2020; Robb et al., 2020).

In addition, we show qualitative comparisons in appendix D, where our model maintains a good generation while StyleGAN2 and baseline are model-collapsed.

The self-supervision methods and generalization ability on D: Apart from the auto-encoding training for D, we show that D with other common self-supervising strategies also boost GAN's performance in our training settings. We test five self-supervision settings, as shown in Table 6, which all brings a substantial performance boost compared to the baseline model. Specifically, setting-a refers to contrastive learning which we treat each real image as a unique class and let D classify them. For setting-b, we train D to predict the real image's original aspect-ratio since they are reshaped to square when fed to D. Setting-c is the method we employ in our model, which

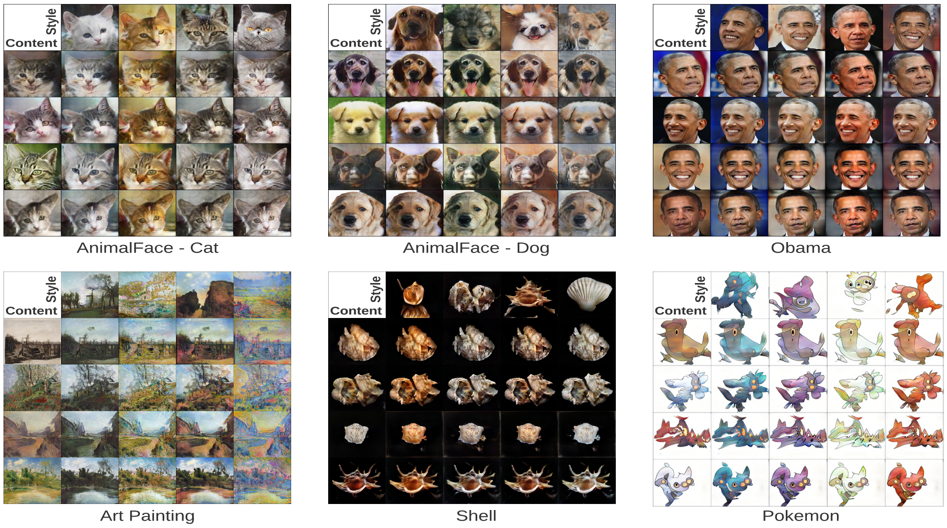

AnimalFace - Cat

AnimalFace - Dog

Obama

Art Painting

Shell

Pokemon

Figure 7: **Style-mixing results** from our model trained for only 5 hours on single GPU.

trains D as an encoder with a decoder to reconstruct real images. To better validate the benefit of self-supervision on D, all the testings are conducted on full training sets with 10000 images, with a batch-size of 8 to be consistent with Table 4. We also tried training with a larger batch-size of 16, which the results are consistent to the batch-size of 8.

Interestingly, according to Table 6, while setting-c performs the best, combining it with the rest two settings lead to a clear performance downgrade. The similar behavior can be found on some other self-supervision settings, e.g. when follow Chen et al. (2019) with a ”rotation-predicting” task on art-paintings and FFHQ datasets, we observe a performance downgrade even compared to the baseline model. We hypothesis the reason being that the auto-encoding forces D to pay attention to more areas of the input image, thus extracts a more comprehensive feature-map to describe the input image (for a good reconstruction). In contrast, a classification task does not guarantee D to cover the whole image. Instead, the task drives D to only focus on small regions because the model can find class cues from small regions of the images. Focusing on limited regions (i.e., react to limited image patterns) is a typical overfitting behavior, which is also widely happening for D in vanilla GANs. More discussion can be found in appendix B.

Style mixing like StyleGAN. With the channel-wise excitation module, our model gets the same functionality as StyleGAN: it learns to disentangle the images' high-level semantic attributes (style and content) in an unsupervised way, from G's conv-layers at different scales. The style-mixing results are displayed in Fig. 7, where the top three datasets are 256×256 resolution, and the bottom three are 1024×1024 resolution. While StyleGAN2 suffers from converging on the bottom high-resolution datasets, our model successfully learns the style representations along the channel dimension on the “excited” layers (i.e., for feature-maps on 256×256, 512×512 resolution). Please refer to appendix A and C for more information on SLE and style-mixing.

5 Conclusion

We introduce two techniques that stabilize the GAN training with an improved synthesis quality, given sub-hundred high-fidelity images and a limited computing resource. On thirteen datasets with a diverse content variation, we show that a skip-layer channel-wise excitation mechanism (SLE) and a self-supervised regularization on the discriminator significantly boost the synthesis performance of GAN. Both proposed techniques require minor changes to a vanilla GAN, enhancing GAN's practicality with a desirable plug-and-play property. We hope this work can benefit downstream tasks of GAN and provide new study perspectives for future research.

REFERENCES

Rameen Abdal, Yipeng Qin, and Peter Wonka. Image2stylegan: How to embed images into the stylegan latent space? In *Proceedings of the IEEE international conference on computer vision*, pp. 4432–4441, 2019.

Martin Arjovsky and Léon Bottou. Towards principled methods for training generative adversarial networks. In *International Conference on Learning Representations*, 2017.

Martin Arjovsky, Soumith Chintala, and Léon Bottou. Wasserstein generative adversarial networks. In *International conference on machine learning*, pp. 214–223. PMLR, 2017.

David Berthelot, Thomas Schumm, and Luke Metz. Began: Boundary equilibrium generative adversarial networks. *arXiv preprint arXiv:1703.10717*, 2017.

Andrew Brock, Jeff Donahue, and Karen Simonyan. Large scale GAN training for high fidelity natural image synthesis. In *International Conference on Learning Representations*, 2019.

Ting Chen, Xiaohua Zhai, Marvin Ritter, Mario Lucic, and Neil Houlsby. Self-supervised gans via auxiliary rotation loss. In *Proceedings of the IEEE Conference on Computer Vision and Pattern Recognition*, pp. 12154–12163, 2019.

Yann N Dauphin, Angela Fan, Michael Auli, and David Grangier. Language modeling with gated convolutional networks. In *International conference on machine learning*, pp. 933–941, 2017.

Emily L Denton, Soumith Chintala, Rob Fergus, et al. Deep generative image models using a laplacian pyramid of adversarial networks. In *Advances in neural information processing systems*, pp. 1486–1494, 2015.

Ahmed Elgammal, Marian Mazzone, et al. Artists, artificial intelligence and machine-based creativity in playform. *Artnodes*, (26):1–8, 2020.

Ian Goodfellow, Jean Pouget-Abadie, Mehdi Mirza, Bing Xu, David Warde-Farley, Sherjil Ozair, Aaron Courville, and Yoshua Bengio. Generative adversarial nets. In *Advances in neural information processing systems*, pp. 2672–2680, 2014.

Priya Goyal, Dhruv Mahajan, Abhinav Gupta, and Ishan Misra. Scaling and benchmarking self-supervised visual representation learning. In *Proceedings of the IEEE International Conference on Computer Vision*, pp. 6391–6400, 2019.

Ishaan Gulrajani, Faruk Ahmed, Martin Arjovsky, Vincent Dumoulin, and Aaron C Courville. Improved training of wasserstein gans. In *Advances in neural information processing systems*, pp. 5767–5777, 2017.

Yong Guo, Qi Chen, Jian Chen, Qingyao Wu, Qinfeng Shi, and Mingkui Tan. Auto-embedding generative adversarial networks for high resolution image synthesis. *IEEE Transactions on Multimedia*, 21(11):2726–2737, 2019.

Kaiming He, Xiangyu Zhang, Shaoqing Ren, and Jian Sun. Deep residual learning for image recognition. In *Proceedings of the IEEE conference on computer vision and pattern recognition*, pp. 770–778, 2016.

Kaiming He, Haoqi Fan, Yuxin Wu, Saining Xie, and Ross Girshick. Momentum contrast for unsupervised visual representation learning. In *Proceedings of the IEEE/CVF Conference on Computer Vision and Pattern Recognition*, pp. 9729–9738, 2020.

Dan Hendrycks, Mantas Mazeika, Saurav Kadavath, and Dawn Song. Using self-supervised learning can improve model robustness and uncertainty. In *Advances in Neural Information Processing Systems*, pp. 15663–15674, 2019.

Martin Heusel, Hubert Ramsauer, Thomas Unterthiner, Bernhard Nessler, and Sepp Hochreiter. Gans trained by a two time-scale update rule converge to a local nash equilibrium. In *Advances in neural information processing systems*, pp. 6626–6637, 2017.

Jie Hu, Li Shen, and Gang Sun. Squeeze-and-excitation networks. In *Proceedings of the IEEE conference on computer vision and pattern recognition*, pp. 7132–7141, 2018.

Xun Huang and Serge Belongie. Arbitrary style transfer in real-time with adaptive instance normalization. In *Proceedings of the IEEE International Conference on Computer Vision*, pp. 1501–1510, 2017.

Xun Huang, Yixuan Li, Omid Poursaeed, John Hopcroft, and Serge Belongie. Stacked generative adversarial networks. In *Proceedings of the IEEE conference on computer vision and pattern recognition*, pp. 5077–5086, 2017.

Longlong Jing and Yingli Tian. Self-supervised visual feature learning with deep neural networks: A survey. *IEEE Transactions on Pattern Analysis and Machine Intelligence*, 2020.

Animesh Karnewar and Oliver Wang. Msg-gan: Multi-scale gradients for generative adversarial networks. In *Proceedings of the IEEE/CVF Conference on Computer Vision and Pattern Recognition*, pp. 7799–7808, 2020.

Tero Karras, Timo Aila, Samuli Laine, and Jaakko Lehtinen. Progressive growing of GANs for improved quality, stability, and variation. In *International Conference on Learning Representations*, 2018.

Tero Karras, Samuli Laine, and Timo Aila. A style-based generator architecture for generative adversarial networks. In *Proceedings of the IEEE conference on computer vision and pattern recognition*, pp. 4401–4410, 2019.

Tero Karras, Miika Aittala, Janne Hellsten, Samuli Laine, Jaakko Lehtinen, and Timo Aila. Training generative adversarial networks with limited data. *arXiv preprint arXiv:2006.06676*, 2020a.

Tero Karras, Samuli Laine, Miika Aittala, Janne Hellsten, Jaakko Lehtinen, and Timo Aila. Analyzing and improving the image quality of stylegan. In *Proceedings of the IEEE/CVF Conference on Computer Vision and Pattern Recognition*, pp. 8110–8119, 2020b.

Anders Boesen Lindbo Larsen, Søren Kaae Sønderby, Hugo Larochelle, and Ole Winther. Autoencoding beyond pixels using a learned similarity metric. In *International conference on machine learning*, pp. 1558–1566. PMLR, 2016.

Jae Hyun Lim and Jong Chul Ye. Geometric gan. *arXiv preprint arXiv:1705.02894*, 2017.

Zachary C. Lipton and Subarna Tripathi. Precise recovery of latent vectors from generative adversarial networks. *ICLR workshop*, 2017.

Bingchen Liu, Kunpeng Song, Yizhe Zhu, Gerard de Melo, and Ahmed Elgammal. Time: Text and image mutual-translation adversarial networks. In *Thirty-Fifth AAAI Conference on Artificial Intelligence*, 2021.

Lars Mescheder, Andreas Geiger, and Sebastian Nowozin. Which training methods for gans do actually converge? In *International conference on machine learning*, pp. 3481–3490. PMLR, 2018.

Takeru Miyato, Toshiki Kataoka, Masanori Koyama, and Yuichi Yoshida. Spectral normalization for generative adversarial networks. In *International Conference on Learning Representations*, 2018.

Sangwoo Mo, Minsu Cho, and Jinwoo Shin. Freeze discriminator: A simple baseline for fine-tuning gans. *arXiv preprint arXiv:2002.10964*, 2020.

Mkhuseli Ngxande, Jules-Raymond Tapamo, and Michael Burke. Depthwisegans: Fast training generative adversarial networks for realistic image synthesis. In *2019 Southern African Universities Power Engineering Conference/Robotics and Mechatronics/Pattern Recognition Association of South Africa (SAUPEC/RobMech/PRASA)*, pp. 111–116. IEEE, 2019.

Maria-Elena Nilsback and Andrew Zisserman. A visual vocabulary for flower classification. In *IEEE Conference on Computer Vision and Pattern Recognition*, volume 2, pp. 1447–1454, 2006.

Atsuhiro Noguchi and Tatsuya Harada. Image generation from small datasets via batch statistics adaptation. In *Proceedings of the IEEE International Conference on Computer Vision*, pp. 2750–2758, 2019.

Adam Paszke, Sam Gross, Soumith Chintala, Gregory Chanan, Edward Yang, Zachary DeVito, Zeming Lin, Alban Desmaison, Luca Antiga, and Adam Lerer. Automatic differentiation in pytorch. 2017.

Alec Radford, Luke Metz, and Soumith Chintala. Unsupervised representation learning with deep convolutional generative adversarial networks. *arXiv preprint arXiv:1511.06434*, 2015.

Esther Robb, Wen-Sheng Chu, Abhishek Kumar, and Jia-Bin Huang. Few-shot adaptation of generative adversarial networks. *arXiv preprint arXiv:2010.11943*, 2020.

Zhangzhang Si and Song-Chun Zhu. Learning hybrid image templates (hit) by information projection. *IEEE Transactions on pattern analysis and machine intelligence*, 34(7):1354–1367, 2011.

Samarth Sinha, Han Zhang, Anirudh Goyal, Yoshua Bengio, Hugo Larochelle, and Augustus Odena. Small-gan: Speeding up gan training using core-sets. *arXiv preprint arXiv:1910.13540*, 2019.

Dustin Tran, Rajesh Ranganath, and David M Blei. Deep and hierarchical implicit models. *arXiv preprint arXiv:1702.08896*, 7(3):13, 2017.

Ngoc-Trung Tran, Viet-Hung Tran, Bao-Ngoc Nguyen, Linxiao Yang, and Ngai-Man Man Cheung. Self-supervised gan: Analysis and improvement with multi-class minimax game. *Advances in Neural Information Processing Systems*, 32:13253–13264, 2019.

Dmitry Ulyanov, Andrea Vedaldi, and Victor Lempitsky. Instance normalization: The missing ingredient for fast stylization. *arXiv preprint arXiv:1607.08022*, 2016.

Ting-Chun Wang, Ming-Yu Liu, Jun-Yan Zhu, Andrew Tao, Jan Kautz, and Bryan Catanzaro. High-resolution image synthesis and semantic manipulation with conditional gans. In *Proceedings of the IEEE conference on computer vision and pattern recognition*, pp. 8798–8807, 2018.

Yaxing Wang, Abel Gonzalez-Garcia, David Berga, Luis Herranz, Fahad Shahbaz Khan, and Joost van de Weijer. Minegan: effective knowledge transfer from gans to target domains with few images. In *Proceedings of the IEEE/CVF Conference on Computer Vision and Pattern Recognition*, pp. 9332–9341, 2020.

Yasin Yazıcı, Chuan-Sheng Foo, Stefan Winkler, Kim-Hui Yap, Georgios Piliouras, and Vijay Chandrasekhar. The unusual effectiveness of averaging in gan training. *arXiv preprint arXiv:1806.04498*, 2018.

Dan Zhang and Anna Khoreva. Pa-gan: Improving gan training by progressive augmentation. 2018.

Han Zhang, Tao Xu, Hongsheng Li, Shaoting Zhang, Xiaogang Wang, Xiaolei Huang, and Dimitris N Metaxas. Stackgan: Text to photo-realistic image synthesis with stacked generative adversarial networks. In *Proceedings of the IEEE international conference on computer vision*, pp. 5907–5915, 2017.

Richard Zhang, Phillip Isola, Alexei A Efros, Eli Shechtman, and Oliver Wang. The unreasonable effectiveness of deep features as a perceptual metric. In *Proceedings of the IEEE conference on computer vision and pattern recognition*, pp. 586–595, 2018.

Junbo Zhao, Michael Mathieu, and Yann LeCun. Energy-based generative adversarial network. *arXiv preprint arXiv:1609.03126*, 2016.

Shengyu Zhao, Zhijian Liu, Ji Lin, Jun-Yan Zhu, and Song Han. Differentiable augmentation for data-efficient gan training. *arXiv preprint arXiv:2006.10738*, 2020.

Jiachen Zhong, Xuanqing Liu, and Cho-Jui Hsieh. Improving the speed and quality of gan by adversarial training. *arXiv preprint arXiv:2008.03364*, 2020.

Jiapeng Zhu, Yujun Shen, Deli Zhao, and Bolei Zhou. In-domain gan inversion for real image editing. *arXiv preprint arXiv:2004.00049*, 2020.

Jun-Yan Zhu, Philipp Krähenbühl, Eli Shechtman, and Alexei A Efros. Generative visual manipulation on the natural image manifold. In *European conference on computer vision*, pp. 597–613. Springer, 2016.